J Mater Sci (2012) 47:486–492
DOI 10.1007/s10853-011-5824-x

Glass reactive sintering as an alternative route for the synthesis of NZP glass–ceramics

Sébastien Chenu · Ronan Lebullenger · Patricia Bénard-Rocherullé · Guillaume Calvez · Olivier Guillou · Jean Rocherullé · Abdessamad Kidari · Mickael J. Pomeroy · Stuart Hampshire

Received: 27 April 2011 / Accepted: 26 July 2011 / Published online: 11 August 2011

Abstract The NZP-type crystal structure allows a large number of ionic substitutions which leads to ceramics with adjustable thermal expansion properties or interesting ionic conductivity. However, NZP is difficult to fabricate into monoliths because it requires both high temperatures and long sintering times. An alternative low temperature route to obtain a tungsten (IV) and tin (IV) containing NZP crystalline phase uses a process of glass reactive sintering of a phosphate glass. Using a microwave oven, a glass with the appropriate composition in the NaPO3–Sn(II)O–W(VI)O3 ternary diagram is prepared by a conventional melting and casting technique. After crushing, the glass powder is pressed at room temperature. The green pellet is cured during various times at temperatures where glass reactive sintering takes place. From XRD and DTA experiments, we have shown that different parameters influence the achievement of NZP phase. Consequently, specific conditions, such as (i) initial glass composition, (ii) equimolar quantities of SnO and WO3, (iii) glass particle size lower than 100 μm, and (iv) curing conducted under air, are required to obtain a glass–ceramic with a single crystalline phase with the NZP-type crystal structure.

S. Chenu · R. Lebullenger · P. Bénard-Rocherullé · G. Calvez · O. Guillou · J. Rocherullé (✉)
UMR CNRS 6226 Sciences Chimiques de Rennes, Université de Rennes 1, 35042 Rennes, France
e-mail: jean.rocherulle@univ-rennes1.fr
URL: http://www.scienceschimiques.univ-rennes1.fr/equipes/verres-et-ceramiques/

A. Kidari · M. J. Pomeroy · S. Hampshire
Materials and Surface Science Institute, University of Limerick, Limerick, Ireland

A. Kidari
Now at CEA, DEN, DTCD, SECM, LDMC, 30207 Bagnols-sur-Cèze Cedex, France

Introduction

The most representative member of the NZP family is $NaZr_2(PO_4)_3$ from which its name is derived. This structure is a three-dimensional arrangement of ZrO_6 octahedra linked to PO_4 tetrahedra by corner sharing oxygens [1]. The general structural formula is $A_nB_m(PO_4)_3$, where A is an alkaline ion or a vacancy [2, 3] and B a transition metal ion or a combination of ions with different valence states (generally +4 like Zr, Ti, Sn, etc.). The interstitial space created in this open framework is occupied by alkali ions and permits fast ion conduction [4]. Materials with the NZP-type crystal structure are often referred to as "NASICONs", an acronym for "Na-Super Ionic CONductors".

The NZP-type structure allows a large number of ionic substitutions which leads to compounds with different properties and various possible applications. Indeed, NZP materials have been known for their potential to be used in anti-thermal shock applications, with low and tuneable thermal expansion [5, 6], and also as candidates for ceramic nuclear waste encapsulation and immobilisation of radionuclides [7, 8] because of their good chemical and thermal stability. These compounds have also found application as catalyst supports for the reduction of NO*x* and for the oxidation of propene to acrolein [9]. The ionic and superionic conductivity is an interesting property for potential solid electrolytes [10, 11].

However, NZP is difficult to fabricate into monoliths using conventional solid state reaction because it requires both high temperatures (higher than 1000 °C) and long sintering times (several tens of hours). An alternative low-temperature route to obtain NZP crystalline phase consists of glass reactive sintering of a phosphate glass.

In this context, a crystalline material with NZP-type structure containing tungsten (IV) and tin (IV) was

synthesized by glass reactive sintering. $NaSn_2(PO_4)_3$ has already been studied by several authors [12–14], but the literature does not mention, until now, NZP compounds with both tungsten and tin.

In this study, we have developed a novel route for the preparation of NZP glass–ceramics. The choice of the initial glass composition is discussed and different experimental parameters (curing atmosphere, particle size, tungsten role, etc.) are investigated using DTA analysis, X-ray powder diffraction, and thermodiffractometry.

Experimental

Glasses in the ternary $NaPO_3$–$Sn^{(II)}O$–$W^{(VI)}O_3$ system were prepared using a microwave oven [15, 16]. The microwave route offers several advantages over conventional methods, the foremost of which are the very short time scales required for the preparation and the homogeneity of the heating. In a typical experiment, required quantities of starting materials, $NaPO_3$ (Aldrich), SnO (99.9% Alfa Aesar), and WO_3 (99+% Aldrich) are placed in a clean silica crucible and exposed to microwave irradiation up to 10 min in a small scale oven (Kerwave®, 2.45 GHz, 750 W nominal power) under a nitrogen flow (150 L h^{-1}). The crucible is covered by a cap of silica that allows the simultaneous transfer of nitrogen and exhaust gas from the melt. This provides a protective atmosphere avoiding oxidation of tin as mentioned in a previous report [17]. Then, the melt is poured between two stainless steel plates and the glass is annealed for 1 h at temperature close to T_g to relieve residual stress before cooling down slowly to room temperature.

The obtained glass is finely crushed and the glass powder is compressed at room temperature under a pressure of 6 MPa in order to form a green pellet. The diameter of this pellet is about 13 mm and thickness is 4–5 mm. This pellet is cured at different times and temperatures where glass reactive sintering takes place to obtain a dense glass–ceramic.

The characteristic temperatures were measured using a TA Instruments SDT 2960 with an overall accuracy expected to be better than 5 °C for this study. The glass samples were contained in a Pt pan and an empty Pt pan was used as the standard. Non-isothermal experiments were performed under various atmospheres (air, nitrogen, oxygen), using a constant weight of 40 mg. A constant heating rate of 10 °C min^{-1} was employed.

The crystalline phases obtained after the heat treatment were analysed by X-ray powder diffraction (XRD). Data were collected at room temperature with a PHILIPS diffractometer (Model PW 1830) using CuK_α radiation ($K_{\alpha1} = 1.5406$ Å, $K_{\alpha2} = 1.5444$ Å) selected with a diffracted-beam graphite monochromator and the Bragg–Brentano optics. The 12–38° (2θ) angular range was scanned in 0.04° (2θ) steps with a counting time set at 2.5 s $step^{-1}$. The ICDD PDF2 database, available in the program search/match from the PC software package X'PERT supplied by PHILIPS, was interrogated in order to identify the crystalline phases.

Non-isothermal crystallization was studied in situ, up to 750 °C in 20 °C increments, by means of the high-temperature X-ray diffraction technique (HTXRD). These thermal-dependence experiments were performed with a Panalytical X-Pert Pro diffractometer using a fast X-celerator detector. The recording conditions were 40 kV, 40 mA for Cu-K_α ($\lambda = 1.5418$ Å), the diagrams were recorded in θ/θ mode. The heating of the samples was performed using an Anton Paar HTK 1200 furnace under flowing air (10 L h^{-1}), with a heating rate of 10 °C min^{-1}. The equilibrium time, during which the diffraction pattern is recorded, is 7 min. The selected angular range being from 10° to 30° it insures satisfactory counting statistics. In addition, a HTXRD kinetic study of the NZP crystallization has been performed at 750 °C using a heating rate of 20 °C min^{-1}. The 2θ range has been changed from 19° to 22° in order to record the (110) and (104) diffraction peaks which exhibit the highest relative intensity values, 100 and 88, respectively. The counting time is 190 s, insuring a similar quality of the counting statistics as for those of the non-isothermal experiments.

Results and discussion

Glass composition

In a previous study [17], we have shown that several glass compositions in the $NaPO_3$–SnO–WO_3 ternary composition diagram were able to crystallize and to give a single crystalline phase, isostructural to $NaSn_2(PO_4)_3$ probably containing tungsten. Indeed, Sn^{4+} and W^{4+} ionic radii are relatively close (0.83 and 0.80 Å, respectively) [18] giving credence to a possible substitution of W^{4+} for Sn^{4+}. In a first step we determined the theoretical composition of the parent glass in order to prepare a NZP glass–ceramic with an equimolar ratio between tin and tungsten.

Figure 1 shows the calculated quantities (in weight %) of different NZP phases which could be obtained from the $(100-2x)NaPO_3$–$xSnO$–xWO_3 glass compositions as functions of the metal oxide content (i.e., x value). The lower curve (data with filled triangles) represents the quantity of pure tin containing phase (i.e., $NaSn_2(PO_4)_3$) and the upper one (data with open square) represents the tin and tungsten (1:1) containing phase (i.e., $NaSnW(PO_4)_3$). Each curve exhibits a maximum at different values of x. As clearly

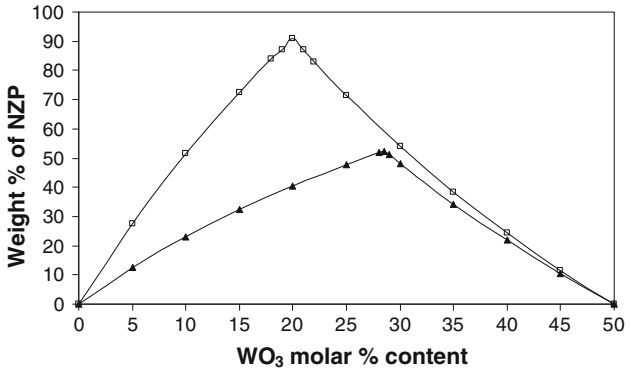

Fig. 1 Theoretical quantities of NZP phase as of function of the WO_3 molar % content. $NaSnW(PO_4)_3$: (*open square*) $NaSn_2(PO_4)_3$: (*filled triangle*)

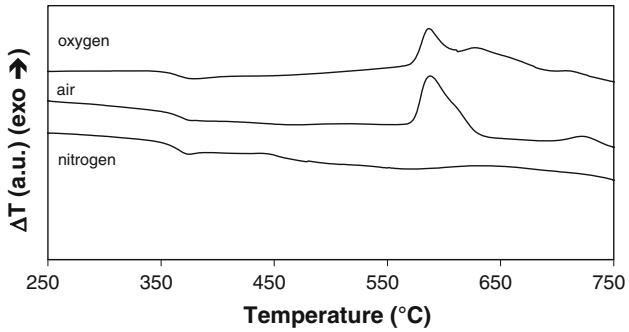

Fig. 2 DTA traces obtained under various atmospheres for the $60NaPO_3$–$20SnO$–$20WO_3$ glass composition

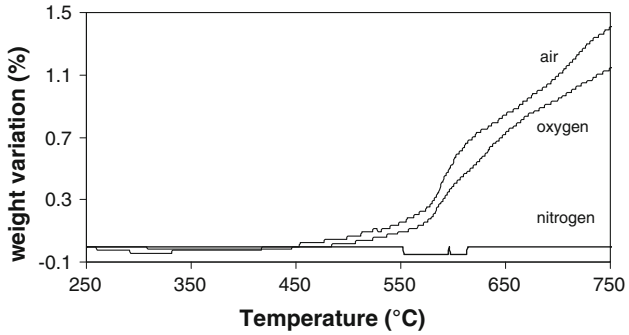

Fig. 3 TGA traces obtained under various atmospheres for the $60NaPO_3$–$20SnO$–$20WO_3$ glass composition

shown, a $60NaPO_3$–$20SnO$–$20WO_3$ glass composition is optimal to obtain the maximum quantity of $NaSnW(PO_4)_3$ phase from glass reactive sintering. This reaches as high as 91 wt% but is limited to this because the amount of sodium present in the glass is higher than the requisite quantity to form this phase. On the contrary, according to the second hypothesis for which only tin is present in the crystalline phase, a lower maximum is reached for a different glass composition (i.e., with 28.5% WO_3), with a maximum of NZP phase of only approximately 48 wt%. Thus, in further experiments, we focused our studies on the $60NaPO_3$–$20SnO$–$20WO_3$ glass composition.

Influence of the atmosphere

Figure 2 represents three DTA curves of $60NaPO_3$–$20SnO$–$20WO_3$ glass powders conducted under different atmospheres (air, nitrogen, and oxygen) up to 750 °C. The particle size of the glass, the sample weight, and the heating rate are kept constant for comparison. A gas flow (4.2 L h^{-1}) is used for DTA experiments performed under nitrogen and oxygen, and experiments under air are made under static air. The glass transition temperature was found to be 367 °C and is independent of the experimental atmosphere. At higher temperatures, different behavior is observed between the experiments performed under air and nitrogen. Under nitrogen, no exothermic event was observed while an exothermic peak around 600 °C is clearly seen under air. This exothermic phenomenon is due to the crystallization of NZP phase as mentioned in a previous study [17]. A similar DTA experiment was also conducted under an oxygen flow. In this case the DTA curve is similar to that obtained under atmospheric air. As a consequence, we assume that an atmosphere containing oxygen is necessary to obtain the NZP phase.

The weight variations were also studied from TGA experiments as shown in Fig. 3. Under air and oxygen, there is an increase in weight, contrary to the experiment conducted under nitrogen. This variation starts at 500 °C and corresponds to oxidation of SnO. Indeed, in the parent glass, tin has formally a (+2) oxidation state while in the NZP phase it becomes (+4). If we consider the direct oxidation of SnO by atmospheric oxygen, the theoretical weight increase is 2.38%. Under air, at 750 °C, 58% of this increase is obtained whereas under oxygen, the variation represents 48%. However, it should be kept in mind that such a difference (i.e., ~10%) corresponds to a low value of the weight difference between the two experiments (i.e., ~0.07 mg). As a consequence, we assume that the presence of oxygen during glass reactive sintering is necessary; nevertheless, the increase in oxygen partial pressure does not allow an improvement in the quantity of NZP phase.

Influence of the glass particle size

The influence of particle size was also studied from DTA–TGA experiments which were performed up to 750 °C, at 10 °C min^{-1} under air. The parent glass is crushed and sieved to obtain nine different particle size ranges (20–40, 40–50, 50–63, 63–80, 80–100, 100–200, 200–315, 315–500, <500 μm).

Figure 4 shows, for each particle size range, the ratio of the experimental weight variation to the theoretical weight variation as determined from TGA experiments. As clearly shown, the NZP phase does not appear for larger particle size (>500 μm) and the occurrence of this phase is strongly correlated with the particle size of the sample, suggestive of a surface related crystallization mechanism. Indeed, a maximum quantity (~58%) is reached for particle sizes lower than 100 μm.

Figure 5 represents the DTA curves for different particle size ranges. The glass transition temperature is always at 367 °C. For particle sizes greater than 315 μm, only one exothermic event is observed at 590 °C. For particle sizes between 315 and 63 μm, a second exothermic phenomenon appears at 700 °C. When the particle size decreases below 63 μm, the second peak is shifted toward lower temperatures and finally links with and broadens the first DTA peak. This is obviously related to the simultaneous phenomena of the oxidation of tin and the crystallization of the NZP phase. As already mentioned in a previous study [19] the presence of two exotherms in the DTA curve for the smaller glass particle sizes does not allow us to conclude that a double step process occurs for the oxidation of tin. In fact, this behavior is typical for any solid–gas reaction [20]. Atmospheric oxygen reacts first with the exterior shell and

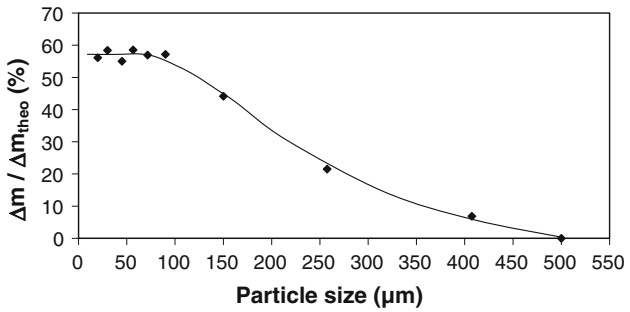

Fig. 4 Relative weight variation as a function of the particle size for the $60NaPO_3$–$20SnO$–$20WO_3$ glass composition

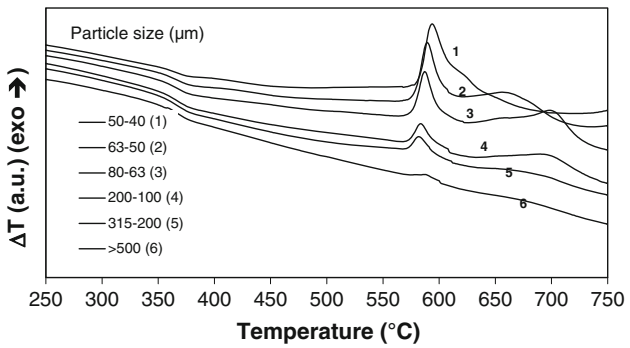

Fig. 5 DTA traces as functions of selected particle sizes

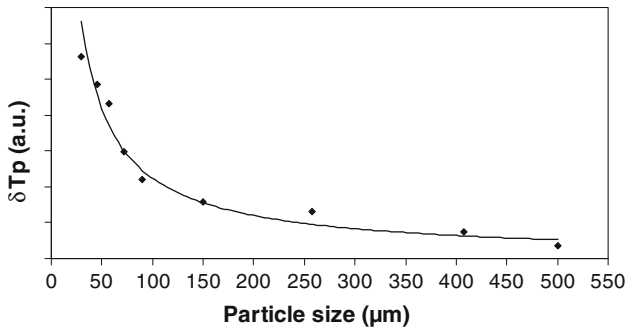

Fig. 6 DTA peak height as a function of the particle size

then a diffusion process inhibits further oxidation of the core of the particle which takes place at higher temperatures. In addition, the derivative TGA curve, not present in Fig. 5, has revealed the presence of two inflexion points at the same temperatures giving credence to this assumption.

It has been previously shown that DTA could be used to determine the dominant crystallization mechanism in glass [21]. In this DTA method, δTp (the maximum height of the DTA crystallization peak) which is expected to be proportional to the total number of nuclei, is plotted as a function of the glass particle size, with both the weight of sample, and the heating rate remaining constant. At constant weight, the ratio of the volume of the sample to its total surface area increases with increasing particle size. For internal dominant crystallization, δTp should increase, whereas for surface dominant crystallization, δTp should decrease with increasing particle size. In the same way, the DTA peak height should give us information about the simultaneous phenomena revealed by the thermal analysis. Figure 6 shows the plot of δTp as a function of the particle size of the sample. As expected, it confirms the strong surface dependence of the simultaneous phenomena and the necessity to use fine glass powders to obtain a maximum of NZP phase during the heat treatment.

The role of tungsten

Different TGA experiments have always shown an increase in weight during the heat treatment. Indeed, if we consider a redox reaction between SnO and WO_3 to obtain Sn^{4+} and W^{4+}, which are the tin and tungsten oxidation states in NZP phase, such a reaction does not require the presence of air and should not exhibit an increase in weight. Therefore, the role of tungsten is questionable and a glass without this element has been prepared to check this hypothesis. A $60NaPO_3$–$40SnO$ glass composition has been synthesised under the same conditions mentioned in the experimental section. Figure 7 illustrates a simultaneous DTA–TGA experiment performed on a glass powder under air. The

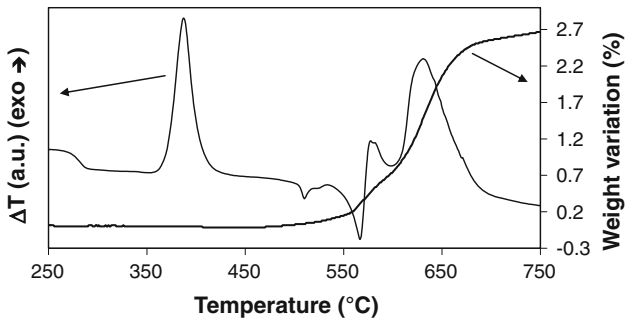

Fig. 7 DTA and TGA traces for a $60NaPO_3$–$40SnO$ glass composition

glass transition temperature is 281 °C. A sharp crystallization peak is observed at 370 °C and two endothermic events at 475 and 550 °C correspond to the melting of different crystalline phases. From 550 °C, one observes an increase of the sample weight up to 2.7% at 750 °C. The DTA curve also shows two maxima at 590 and 640 °C which precisely correspond to the two inflexion points deduced from the shape of the derivative TGA curve (not given in this figure). The thermal behavior of this composition differs from that of the initial glass. It is obvious that the glass melts before the oxidation of tin and the subsequent crystallization. However, the experimental weight gain (2.7%) is lower than theoretical, 5.5%. As a consequence, the complete oxidation reaction is not achieved but an increase in temperature, above 750 °C, could have a deleterious effect on the chemical composition of the residual liquid phase. Afterwards, XRD experiments were conducted on samples which have been heated up to 750 °C and cooled to ambient (see Fig. 8). As expected, several different crystalline phases are present: $NaSn_2(PO_4)_3$, SnO_2 corresponding to ICDD PDF2 card number 49–1198 and 72–1147, respectively, but the major phase remains unidentified.

In addition, two glass compositions with different Sn:W ratios (i.e., 1:3 and 3:1), the $NaPO_3$ content remaining the same, have been heated under air up to 750 °C and then slowly cooled down to room temperature. XRD analysis performed on the $60NaPO_3$–$10SnO$–$30WO_3$ composition has revealed the presence of a NZP phase in association with one or more unidentified crystalline phases. On the contrary, the $60NaPO_3$–$30SnO$–$10WO_3$ composition was not crystallized, even after heating up to 750 °C. All these different experiments lend support to the fact that tungsten oxide is necessary and must be present with the same proportion as SnO in order to obtain a pure NZP phase, without any secondary crystalline phases.

High temperature X-ray diffraction study

The reactivity of the $60NaPO_3$–$20SnO$–$20WO_3$ glass composition has been studied in situ up to 750 °C. Glasses have been crushed and sieved to obtain a particle size of the samples in the range from 40 to 63 μm which insures the completion of the NZP crystallization as shown in Fig. 4.

Figure 9 shows XRD patterns which describe this non isothermal process from 450 to 750 °C. Below 470 °C there are no diffraction peaks, the material being totally amorphous. Crystallization begins at 470 °C with the appearance of a phase which is probably isostructural with $NaSn_2(PO_4)_3$ (ICDD-PDF 2 no. 49-1198). From 470 to 710 °C, the intensities of the NZP diffraction peaks strongly increase; nevertheless, other crystalline phases simultaneously appear. Unfortunately, these secondary phases cannot be identified by interrogation of the ICDD-PDF2 database. Above 710 °C, an increase of temperature allows only the NZP phase to be obtained. Furthermore, an important shift in 2θ ($\sim 0.2°$) is observed between 710 and 750 °C with all NZP diffraction peaks shifted to smaller angles. This phenomenon has two possible causes: a chemical composition change in the NZP-type crystal structure (i.e., tin for tungsten substitution) or a focussing defect of the X-ray incident beam due to a volume change

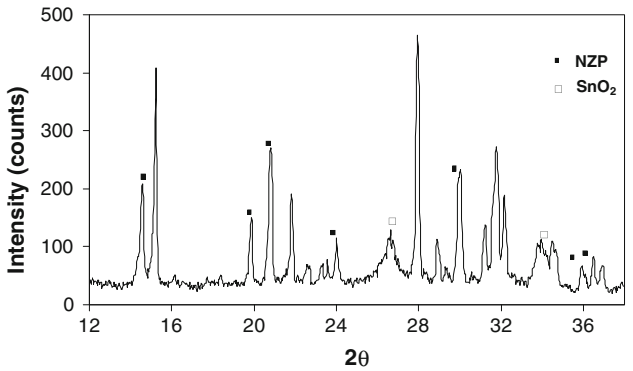

Fig. 8 XRD pattern of a $60NaPO_3$–$40SnO$ glass sample after heating up to 750 °C

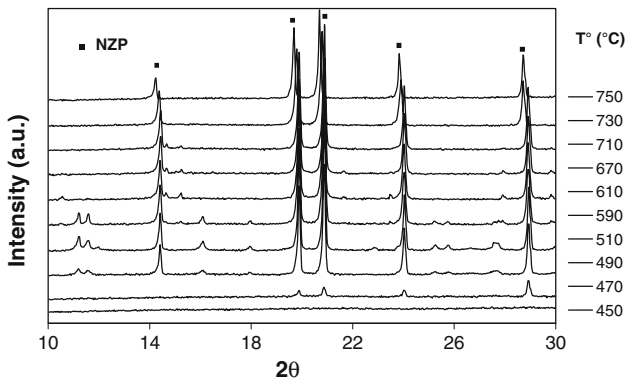

Fig. 9 XRD patterns recorded at various temperatures from 450 to 750 °C for the $60NaPO_3$–$20SnO$–$20WO_3$ glass composition

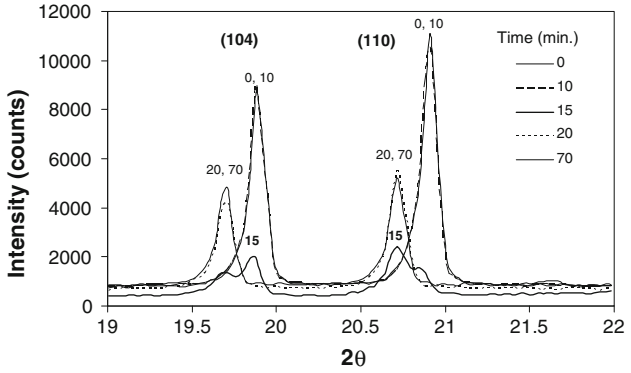

Fig. 10 XRD patterns recorded at 750 °C during various times for the $60NaPO_3$–$20SnO$–$20WO_3$ glass composition

of the sample at high temperature. Consequently, we compared the XRD pattern obtained at 750 °C to the one recorded after cooling down the sample to room temperature, without removing the sample from the diffractometer. The peak positions were exactly the same. Thus, if there is a structural modification, it is irreversible. The sample was then removed from the diffractometer and crushed and a second XRD pattern was recorded. The previous shift disappeared and the peak positions were the same as observed at 710 °C. From these experiments, it can be concluded that the shift observed during heating is due to a focussing defect which is the result of the sintering of the powder in situ within the instrument. This result confirms the general trend observed during the glass–ceramic synthesis, i.e., a densification of the cold pressed pellet on heating.

As mentioned in the experimental section, an XRD kinetic study has been performed at 750 °C. Figure 10 clearly shows that after 20 min at 750 °C, the intensities of the NZP diffraction peaks reach their maxima. An additional heating up to 70 min does not change these intensities. Thus, the NZP crystallization at 750 °C is considered complete after only 20 min. Furthermore, Fig. 10 also shows the peak shift due to the dimensional change of the sample previously mentioned. After heating for 10 min, the peaks have not changed position in relation to those observed at zero time. The diffraction pattern obtained after a heating time of 15 min shows the splitting into two diffraction peaks. Indeed, this phenomenon is due to the recording duration for a diffraction pattern (i.e., 190 s). During this time, the glass–ceramic is sintering and therefore shrinking in a continuous way, leading first to a broadening of the diffraction peaks followed by their splitting and finally the occurrence of two well-defined diffraction peaks with a similar shift to that seen in the case of the non-isothermal XRD study. The peak positions do not change anymore after 20 min. Consequently, one can assume that the duration of the reactive sintering reaction does not exceed 20 min at 750 °C.

Conclusion

This study demonstrates that W(IV) and Sn (IV) containing NZP glass–ceramics can be obtained by a glass reactive sintering process. This is an alternative route that consumes less energy and time when compared to the conventional solid state reaction process. A phosphate-based glass, with the appropriate chemical composition, is synthesized in less than 10 min by using a microwave heating device; then the powdered glass is cold pressed and heated to 750 °C during 20 min giving a glass–ceramic containing a single NZP crystalline phase. This glass reactive sintering has been studied by means of DTA and XRD experiments. Different parameters have been optimized; it has been shown that three parameters are critical for obtaining a pure NZP phase. It is necessary to have (i) a fine powder (<100 μm), because the crystallization is controlled by a surface dominant mechanism, (ii) the presence of oxygen during sintering (oxygen contained in air is sufficient), and (iii) the presence of tungsten oxide in equimolar ratio with SnO in the initial glass. Moreover, the temperature must be strictly superior to 710 °C to obtain a NZP glass–ceramic without any secondary crystalline phases. Further studies are in progress to refine the crystal structure and to determine precisely the chemical composition. As this type of structure is well-known for generating high alkali ionic conductivity, the use of these glass–ceramics as solid electrolytes can be envisaged.

References

1. Hagman LO, Kierkegaard P (1968) Acta Chem Scand 22:1822
2. Subba Rao GV, Varadaraju UV, Thomas KA, Sivasankar B (1987) J Solid State Chem 70:101
3. Leclaire A, Borel MM, Grandin A, Raveau B (1989) Acta Cryst C 45:699
4. Goodenough JB, Hong HY-P, Kafalas JA (1976) Mater Res Bull 11:203
5. Oikonomou P, Dedeloudis C, Stournaras CJ, Ftikos C (2007) J Eur Ceram Soc 27:1253
6. Breval E, McKinstry HA, Agrawal DK (2000) J Mater Sci 35:3359. doi:10.1023/A:1004828917908
7. Buvaneswari G, Varadaraju UV (2000) Mater Res Bull 35:1313
8. Roy R, Vance ER, Alamo J (1982) Mater Res Bull 17:585
9. Yamamoto K, Kasuga T, Abe Y (1997) J Am Ceram Soc 80:822
10. Zhou M, Ahmad A (2007) Sensors Actuators B Chem 122:419
11. Lisdat F, Miura N, Yamazoe N (1996) Sensors Actuators B Chem 30:195
12. Rodrigo JL, Alamo J (1991) Mater Res Bull 26:475
13. Breval E, Harshé G, Agrawal DK, Limaye SY (1995) J Mater Sci Lett 14:728

14. Vaidhyanathan B, Agrawal DK, Roy R (2004) J Am Ceram Soc 87:834
15. Vaidhyanathan B, Ganguli M, Rao KJ (1994) J Solid State Chem 113:448
16. Ghussn L, Martinelli JR (2004) J Mater Sci 39:1371. doi:10.1023/B:JMSC.0000013899.75724.e1
17. Chenu S, Lebullenger R, Rocherullé J (2010) J Mater Sci 45:6505. doi:10.1007/s10853-010-4739-2
18. Shannon RD (1976) Acta Cryst A32:751
19. Chenu S, Rocherullé J, Lebullenger R, Merdrignac O, Cheviré F, Tessier F, Oudadesse H (2010) J Non Cryst Solid 356:87
20. Muñoz F, Pascual L, Durán A, Rocherullé J, Marchand R (2006) J Eur Ceram Soc 26:1455
21. Ray CS, Day DE (1990) J Am Ceram Soc 73:439